Production and Characterization of Hybrid BEH-PPV/PEO Conjugated Polymer Nanofibers by Forcespinning™

Simon Padron,[1] Richard Patlan,[1] Jose Gutierrez,[2] Nestor Santos,[2] Thomas Eubanks,[2] Karen Lozano[1]

[1]*Mechanical Engineering Department, The University of Texas Pan American, Edinburg, Texas 78539*
[2]*Chemistry Department, The University of Texas Pan American, Edinburg, Texas 78539*

Received 27 July 2011; accepted 27 October 2011
DOI 10.1002/app.36420
Published online in Wiley Online Library (wileyonlinelibrary.com).

ABSTRACT: The fabrication of hybrid poly(2,5-bis(2′-ethyl-hexyl)-1,4-phenylenevinylene) (BEH-PPV) and polyethylene oxide (PEO) nanofibers is reported. Nanofibers were created using a novel production method that uses centrifugal rather than electrostatic force to produce nanofibers. The nanofiber production method exhibits high yield production of nanofibers enabling mass-production capabilities. Thermo-physical characterization and X-ray diffraction of bulk PEO and BEH-PPV was conducted, and the results are compared with the produced hybrid nanofibers. © 2012 Wiley Periodicals, Inc. J Appl Polym Sci 000: 000–000, 2012

Key words: nanofiber; differential scanning calorimetry (DSC); conjugated polymers

INTRODUCTION

In recent years, conjugated polymers have attracted interest for their potential applications in photovoltaic cells,[1,2] light-emitting diodes,[3,4] optoelectric transistors,[5,6] electromagnetic shielding fabrics, chemical sensors,[7–10] and as biocompatible materials.[11–13] Polyphenylenevinylene (PPV) derivatives are types of conjugated polymers that not only possess semiconducting characteristics but also exhibit photoluminescent properties. Poly(2,5-bis(2′-ethyl-hexyl)-1,4-phenylenevinylene) (BEH-PPV), a polyphenylenevinylene derivative, is a soluble conjugative polymer that has a bulk wavelength emission peak near 590 nm.

The photoluminescent qualities of conjugated polymers like PPVs make them attractive materials for applications in light emitting diodes. The low voltages required to activate the polymers and their flexible properties have allowed for technologies such as flexible thin displays.[14] Conjugated polymers are also promising as gain media for optically pumped microlasers due to the small amount of material needed to produce photoluminescence.[15,16] The capability to produce devices for optical communication is essential for the advancement and realization of optical computing, such devices include optoelectric transistor devices.[5]

Biomedical applications for conjugated polymers have been an area of interest due to the biomimetic capabilities of such materials and their biocompatibility.[17] Conjugated polymers have been proposed as an actuating material for uses in steerable catheters[19,20] and microvalve actuators.[21] The special properties that make conjugated polymers attractive include: their ability to be actuated with low voltages, the large strains and stresses that they exhibit, their weight to power ratio, ability to operate in electrolytes, including body fluids, and their ability to operate at room or body temperatures.[14]

Mazzoldi and De Rossi[19] have proposed the use of conjugated polymers to produce actuation in steerable catheters for minimally invasive surgery. The application reported involves the use of catheters as endoscopes that can be navigated within blood vessels. This requires that the catheters be small in size, provide large angles of actuation, and have response times in the order of seconds.[20] The actuation capabilities of conjugated polymers have also been used by Pettersson et al. to develop a microvalve used to control fluid flow in microchannels. The microvalve is composed of a rigid plate, which prohibits or allows the passage of fluid through the actuation of a conjugated polymer hinge.[21] Jager et. al[22] have fabricated cell clinics, which can be opened or closed by means of a conjugated polymer hinge. This consists of a microcavity

Correspondence to: S. Padron (spadron17@gmail.com or spadronz@broncs.utpa.edu).

Contract grant sponsor: National Science Foundation; contract grant number: DMR 0934157.

Contract grant sponsor: U.S. Army Research Laboratory and the U.S. Army Research Office; contract grant number: W911NF-08-1-0353.

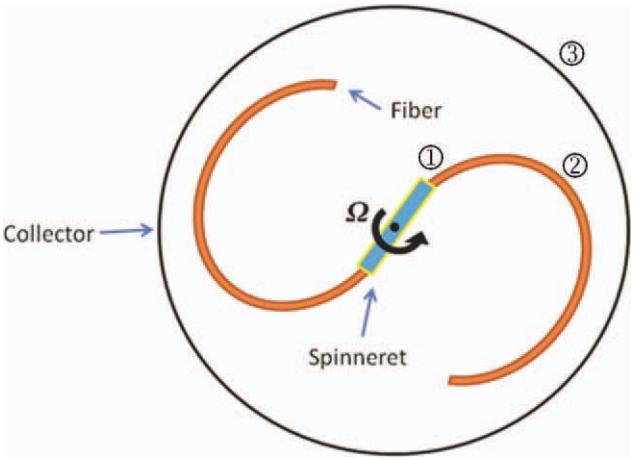

Figure 1 Forcespinning™ fiber production process: φjet exit, (fiber diameter reduction, λfiber collection. [Color figure can be viewed in the online issue, which is available at wileyonlinelibrary.com.]

(100 mm × 100 mm) that can be closed with a lid, which is activated by the conjugated polymer, polypyrrole.

Many of the proposed applications for conjugated polymer materials rely on the ability to manufacture them into nanofibers, which enhances their mechanical, electrical, and optical properties. For instance, it has been demonstrated that the induced orientation could lead to polarized photoluminescence and high-carrier mobility.[23] Conjugated polymer nanofibers also hold promise for serving as nanowires, a crucial component for the development of nanoelectronics.[24,25] Zhu et al.[26] were able to produce hybrid poly[2-methoxy-5-(2′-ethyl-hexyloxy)-1,4-phenylene vinylene] (MEH-PPV)/polyethylene oxide (PEO) nanofibers with average diameters between 500 and 700 nm using the electrospinning method. The solutions were prepared with a tetrahydrofuran (THF)/ Dimethylformamide (DMF) solvent mix at various concentrations. The produced nanofibers were studied for fluorescence and compared with spin-coated MEH-PPV/PEO thin films. At low concentrations of PPV, the nanofibers enhanced the fluorescence of the materials, when compared with the thin films. The difficulty to dissolve PPV and its derivatives has also led to the use of a coaxial electrospinning method.[27–29] Zhao et al. prepared coaxial fibers by dissolving MEH-PPV in chlorobenzene and PVP in 1,2-dichloroethane. The fibers produced with this method showed a core-shell structure with PVP as the shell and MEH-PPV within the core.

A common problem associated with the production of nanofibers using methods such as electrospinning is the inherent low solubility of conjugated polymers, the low yields obtained, and the restrictions imposed by the electrostatic fields. Forcespinning™ has proven successful as an alternative way of producing polymer nanofibers. Unlike electrospinning, which draws fibers through the use of electrostatic force, Forcespinning™ uses centrifugal force, which allows for a significant increase in yield and ease of production. No electric fields are needed; therefore, restrictions imposed on materials with low dielectric constants are eliminated (i.e., fluoropolymers). The Forcespinning™ process begins by first loading the desired solution into a special spinneret. The spinneret is then made to spin at a certain angular velocity. The rotating forces expel the solution, producing a continuous fiber that spirals and expands outward until it is eventually collected either on a substrate, in between vertical prongs (designed collector), or as aligned fibers into a yarn by a spooling mechanism. A schematic depicting the Forcespinning™ procedure is shown in Figure 1. Sarkar et al.[30] present a detailed description of the Forcespinning™ apparatus. To successfully produce nanofibers and determine the final fiber diameter, various parameters must be controlled. The modeling of the fiber formation requires the determination of the trajectory and final diameter size, which are based on the angular velocity of the spinneret, viscoelastic properties of the polymer, collector diameter, radius of the needle orifice, and solvent evaporation rate. In certain cases, the effects of gravity may also have an effect on the formation of the fibers. Using a rotating reference for the coordinate system, the governing equations of the system may be described by the continuity equation:

$$\nabla \bullet u = 0 \tag{1}$$

where $\boldsymbol{u}$ is the relative velocity of the fiber jet, and the Cauchy momentum equations:

$$\frac{\partial \boldsymbol{u}}{\partial t} + (\boldsymbol{u} \bullet \nabla)\boldsymbol{u} = -\frac{\nabla P}{\rho} + \boldsymbol{g} + \frac{\nabla \mathbf{T}}{\rho} - \omega \times (\omega \times \mathbf{r}) - 2\omega \times \boldsymbol{u} \tag{2}$$

where P is the pressure, $\boldsymbol{g}$ is the gravity vector, $\boldsymbol{T}$ is the stress tensor, ω is the angular velocity of the spinneret, and $\mathbf{r}$ is a position vector describing a point along the fiber. The viscoelastic component depends on the polymer properties and is most basically described by the stress tensor, strain-rate tensor, polymer viscosity, and polymer relaxation time. The nondimensional form of the equations provides some important dimensionless numbers that give the ratios between the various forces in the system. Some of these important dimensionless numbers include the Reynolds, Froude, Capillary, Rossby, and Deborah numbers. These values give the ratio of inertial forces to viscous forces along with the fiber's inertial force to gravitational force,[31] inertial

force to surface tension,[31] inertial force to Coriolis force,[32] and polymer relaxation to flow time.[31]

Reported here is the production of BEH-PPV nanofibers. The results show a high yield of nanofibers, when compared with other production methods and prove the ability to forcespin hybrid conjugated polymer nanofibers. Blends of BEH-PPV and PEO were produced at concentrations of 0, 0.5, 1.0, 2.5, 5.0, and 10.0 wt % BEH-PPV to PEO. PEO was chosen for its viscoelastic properties, which are well suited for spinning and because it is soluble in chloroform, which is also a good solvent for BEH-PPV. Also reported are the yields and the diameter of the resulting fiber at various concentrations and spinning rpm. The fibers were analyzed using thermo-physical characterization and X-ray diffraction (XRD).

EXPERIMENTAL SETUPS

Materials and reagents

PEO with an average molecular weight of 900,000 g mol^{-1}, obtained from Sigma-Aldrich, and chloroform (99.9%), obtained from Fox Scientific, were used.

Synthesis of BEH-PPV precursor monomer and polymerization

BEH-PPV was synthesized, according to the literature, with slight modifications.[33–35]

1,4-bis-(2′-ethylhexyloxy)benzene (1)

Potassium hydroxide (28.5 g, 509 mmol) was dissolved in Dimethyl sulfoxide (DMSO) (200 mL) in a 500 mL three-necked round bottom flask under a blanket of nitrogen. Hydroquinone (20 g, 182 mmol) was then added, and the mixture was stirred for 30 min at room temperature, followed by addition of 2-ethylhexylbromide (92.3 g, 478 mmol). The reaction mixture was stirred under nitrogen at room temperature overnight. The reaction mixture was partitioned between water and diethyl ether, the layers were separated. The organic layer was washed three times with 100 mL of DI water, dried over magnesium sulfate, and the solvent was removed under reduced pressure. The oily residue was purified by column chromatography (basic alumina, hexanes) to afford 47 g (78% yield) of a yellow oil. ^{1}H-NMR ($CDCl_3$, 270 MHz): δ 6.86 (s, 4H), 3.84–3.81 (d, 4H), 1.8–1.65 (m, 2H), 1.6–1.2 (m, 18H), 0.97–0.95 (t, 12H). ^{13}C-NMR ($CDCl_3$, 270 MHz): δ 153.5, 115.4, 71.2, 39.6, 30.6, 28.9, 23.9, 23.2, 14.2, 11.2.

1,4-dibromo-2,5-bis-(2′-ethylhexyloxy) xylene (2)

1 (45 g, 135 mmol) was added to a suspension of paraformaldehyde (19.4 g, 647 mmol) and glacial acetic acid (25 mL) in a 250 mL round bottom flask. The suspension was stirred for 15 min at room temperature and then 117 mL of 33% hydrogen bromide in acetic acid (646 mmol) were added at once. The reaction was then heated to 80°C for 5 h. The reaction mixture was cooled to room temperature, and crude was partitioned between water and chloroform. The aqueous layer was back-extracted with chloroform, and the organic phase washed with 7% sodium carbonate three times. The organic phase was dried over magnesium sulfate, followed by the removal of the solvent under reduced pressure. Crystallization from isopropyl alcohol afforded 23 g (42% yield) of a white solid; m.p. = 63.5–65°C. ^{1}H-NMR ($CDCl_3$, 270 MHz): δ 6.84 (s, 2H), 4.51 (s, 4H), 3.91–3.82 (d, 4H), 1.8–1.65 (m, 2H), 1.6–1.20 (m, 18H), 0.97–0.94 (t, 12H). ^{13}C-NMR ($CDCl_3$, 270 MHz): δ 138.3, 150.7, 127.4, 115, 71.2, 39.6, 30.7, 29.2, 24.1, 23.1, 14.2, 11.1.

Polymerization procedure. The PPV derivatives were synthesized via "reversed" Gilch polymerization (i.e., addition of the monomer solution to a potassium *tert*-butoxide/initiator solution).

Poly[bis-2,5-(2′-ethylhexyloxy)]-1,4-phenylenevinylene, BEH-PPV

Weighing and transfer of the reagents was performed inside a nitrogen-filled glove box. Potassium *tert*-butoxide (1.47 g, 13 mmol) and *p*-methoxyphenol (8.6 mg, 2.4 mol %) were dissolved in anhydrous THF (120 mL) in a 250 mL round bottom flask equipped with magnetic stirring, and it was then removed from the glove box. The mixture was stirred at room temperature. BEH-PPV monomer (1.5 g, 2.9 mmol) was dissolved in anhydrous THF (10 mL) and was injected at a rate of 20 mL h^{-1} using a KDS (series 200) syringe-pump. Stirring and cooling was continued 1 h after monomer addition was complete. The red polymer was collected on a Millipore Durapore® 0.45 μm membrane filter after precipitation from methanol and dried under vacuum overnight at 50°C. The red polymer strands were collected and dried under vacuum to give 0.83 g (80% yield) of BEH-PPV. ^{1}H-NMR (270 MHz, $CDCl_3$): δ 7.75–7.41 (d, 1.2H), 4.27–3.75 (t, 4H), 1.93–1.73 (t, 2H), 1.70–0.45 (m, 28H). FTIR (polymer film) (cm^{-1}): 2974, 2731, 2668, 2601, 2316, 2221, 2031, 1830, 1804, 1692, 1586, 772, 723. UV-visible absorption λmax_{CHCl3}: 505 nm; photoemission λmax_{CHCl3}: 557 nm. TGA_{Td}: 368°C (onset, 5% weight loss). The molecular structure of the synthesized BEH-PPV is shown in Figure 2.

Sample preparation

The hybrid polymer solution was prepared by dissolving BEH-PPV and PEO in chloroform. To ensure

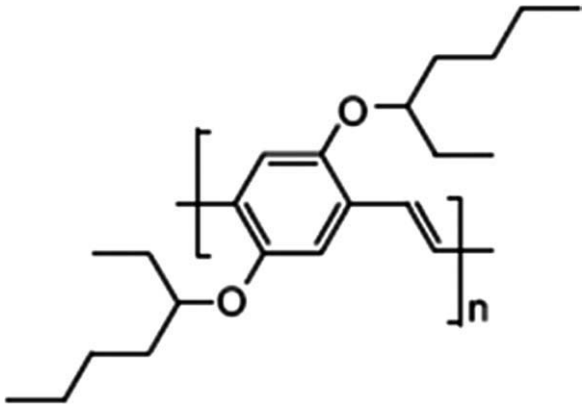

Figure 2 BEH-PPV molecular structure.

a thoroughly mixed solution, the BEH-PPV polymer and the chloroform solvent were first mixed through sonication for 5 h. Afterward, the necessary PEO was added to the solution and mechanically stirred. To determine the effects of BEH-PPV concentrations on the hybrid nanofibers, six different solutions were prepared at 0, 0.5, 1.0, 2.5, 5.0, and 10.0 wt % of BEH-PPV to PEO, as shown in Table I. All solutions were kept at 1.5 wt % of PEO to chloroform.

Nanofiber production

Fibers were forcespun using a prototype Cyclone Forcespinning™ machine. The BEH-PPV/PEO solutions were prepared by injecting them into a specialized cylindrical spinneret holding 1 mL of polymer solution. The fibers were collected using a 10 pronged collector, as shown in Figure 3(a), forming a nanofiber mesh. Each concentration was successfully forcespun at rotational speeds ranging from 2000 to 7000 rpm at times ranging from 10 s at higher speeds to 30 s at the lower speeds. The collected nanofiber mesh and the materials used for production are shown in Figure 3(a,b), respectively.

Nanofiber characterization

The morphology of the nanofibers was analyzed using the Zeiss EVO LS 10 Scanning Electron Microscope (SEM), while thermal characterization was

TABLE I
Concentrations of Solutions Prepared with a Constant 1.5 wt % of PEO to Chloroform

Sample	PEO (wt %)	BEH-PPV (wt %)
1	100	0
2	99.5	0.5
3	99.0	1.0
4	97.5	2.5
5	95.0	5.0
6	90.0	10.0

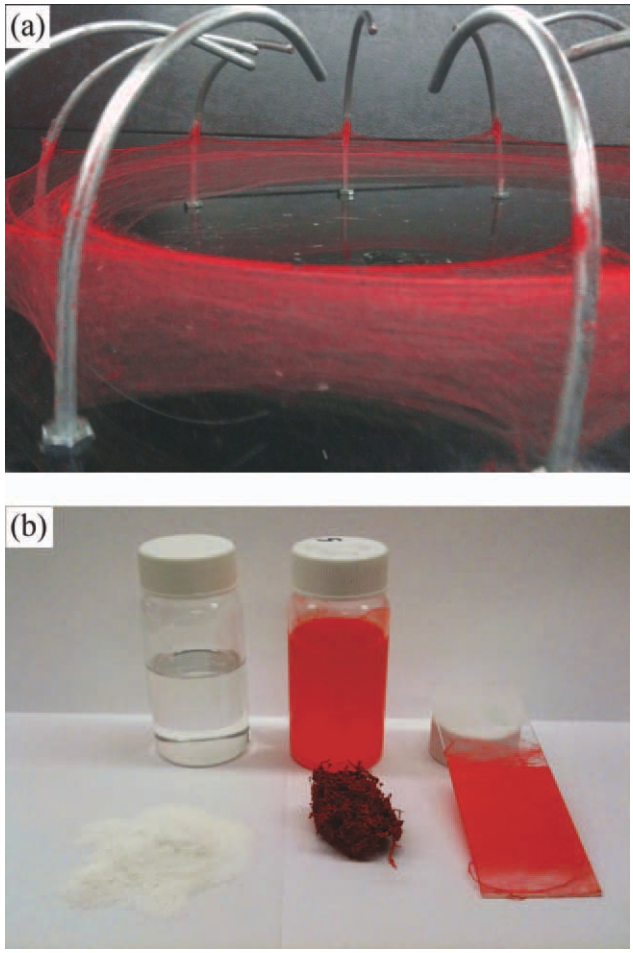

Figure 3 (a) Nanofibers produced with 1 mL of BEH-PPV/PEO solution. (b) Materials used in the production of nanofibers include PEO (white powder), BEH-PPV (red polymer), BEH-PPV in chloroform (container), and resulting nanofibers obtained from solution. [Color figure can be viewed in the online issue, which is available at wileyonlinelibrary.com.]

Figure 4 SEM micrograph of BEH-PPV nanofibers. [Color figure can be viewed in the online issue, which is available at wileyonlinelibrary.com.]

TABLE II
Yield production of BEH-PPV/PEO Fibers in Chloroform Solvent for 1 mL Samples

Speed (RPM)	Pure PEO	0.5 wt % BEH-PPV	1.0 wt % BEH-PPV	2.5 wt % BEH-PPV	5.0 wt % BEH-PPV	10 wt % BEH-PPV
2000	High	Medium	Medium	Medium	–	–
2500	High	Medium	Medium	Medium	High	High
3000	Medium	Medium	Medium	Medium	High	High
4000	Poor	Medium	Low	Low	High	Medium
5000	Poor	Low	Low	Low	Medium	Poor
6000	–	Low	Low	Poor	Poor	–
7000	–	Poor	Poor	–	–	–

performed using the TA Instruments Q100 Differential Scanning Calorimeter (DSC). The nanofiber samples were heated from room temperature at a rate of 5°C min^{-1} to 300°C, held isothermal for 10 min, and cooled at a rate of 5°C min^{-1} to room temperature under nitrogen atmosphere. For XRD analysis, The Bruker AXS D8 Discover Diffractometer was used. The samples were scanned through a range of 15°–70° 2θ angles using a 2D-detector.

RESULTS AND DISCUSSION

The concentration of BEH-PPV present in the solution had a significant effect on the diameter of the fibers obtained. SEM revealed that the optimum BEH-PPV concentration for nanofiber formation was 5 wt %, with an average fiber diameter of 570 nm at a speed of 4000 rpm as observed in Figure 4. The fiber production rate was over 1 g min^{-1} per nozzle, this yield is significantly higher than lab scale electrospinning apparatus, where the system operates at about 0.1 g h^{-1} (considering typical feeding rates of hundreds of mL min^{-1}). In this study, the final product consisted of long, individual nanofibers arranged into free-standing nonwoven mats.

Other parameters are also seen to affect the system as the fiber size does not seem to follow a visible correlation between BEH-PPV concentration and fiber yield and fiber size, as seen from Table II. Work into the modeling of the Forcespinning™ method is currently being conducted to further understand the process. The results show that increasing the rotational speed reduces the fiber diameters until a certain threshold is reached, during which fiber break-up occurs, thus preventing fiber size reduction and increasing the fiber diameter. Higher speeds reduce nanofiber yield due to rotational forces, which impede fiber formation and promote beading. The driving factors determining fiber formation and break-up are the viscosity and surface tension of the forcespun solutions. Therefore, when the viscosity of the solutions is too low, the dominant factor becomes the surface tension.[36] The introduction of BEH-PPV had a mixed effect on the yield and final size of the fibers. The hybrid nanofibers were able to be forcespun at higher speeds with high yields at 5 and 10 wt %. The samples with bold font were those that yielded submicron-nanofibers. To obtain nanofibers, the angular velocity must first be high enough to overcome the viscosity and surface tension of the material. Afterward, the collector must be at an appropriate distance so that the fiber is able to reach the collector. As the angular velocity is increased, the nanofiber diameters have a decreasing trend; however, once a critical angular velocity (dependant on viscoelastic properties of the material) is reached the forces become too large and fiber break-up begins to occur. It is after this critical angular velocity that the solutions begin to be expelled as drops instead of fibers. This is why increasing the angular velocities past the nanofiber formation speeds does not produce finer fibers.

To determine the average diameter sizes, measurements were taken of at least 100 fibers. The largest range of fiber diameter was obtained from the pure PEO nanofibers, with an average diameter of 650 nm. Comparing these results with the aqueous PEO samples obtained in Sarkar et al.,[30] it can be

TABLE III
Measured Fiber Diameters at Varying Concentrations and Speed

Speed (rpm)	0.5% BEH-PPV	1% BEH-PPV	2.5% BEH-PPV	5% BEH-PPV	10% BEH-PPV
2000	1 μm	2 μm	1.5 μm	–	–
2500	1.5 μm	1 μm	2 μm	1 μm	2 μm
3000	1 μm	620 nm	720 nm	1 μm	1 μm
4000	1 μm	–	1 μm	570 nm	–
5000	–	–	–	580 nm	–

TABLE IV
Average Fiber Diameter and Standard Deviation of Samples with Higher Yield

Polymer solutions	Average fiber diameters	Sample standard deviation
1 wt % BEH-PPV at 3000 rpm	620 nm	140 nm
2.5 wt % BEH-PPV at 3000 rpm	720 nm	120 nm
5 wt % BEH-PPV at 4000 rpm	570 nm	120 nm
5 wt % BEH-PPV at 5000 rpm	580 nm	180 nm
Pure PEO sample at 2000 rpm	650 nm	170 nm

deduced that the evaporation rate of the chloroform has a negative effect on the final diameter size, with the chloroform samples being approximately twice as large on average than the water-based PEO solutions. The smallest average diameter of the fibers was obtained from the 5.0 wt % BEH-PPV sample at 4000 rpm as shown in Tables III and IV.

The DSC results are summarized in Table V. Melting and crystallization curves were analyzed for all samples including bulk PEO. Slight melting point depression is observed in the presence of 0.5% to 2.5% BEH-PPV. Crystallization also occurs at slightly higher temperature, small amounts of PPV seem to act as a weak nucleating agent on PEO. However, at higher concentrations, 5% and 10% BEH-PPV crystallization occurs at lower temperatures, where now the PPV is acting as a hindrance to crystallization, given the incompatibility of the systems.

XRD curves show that the incorporation of BEH-PPV onto the crystalline PEO does not affect its crystal lattice. However, addition of BEH-PPV causes a slight increase in the signal occurring at ca. 20°. The effect of BEH-PPV concentration on the signal intensity seems rather aleatory as can be observed from Figure 5.

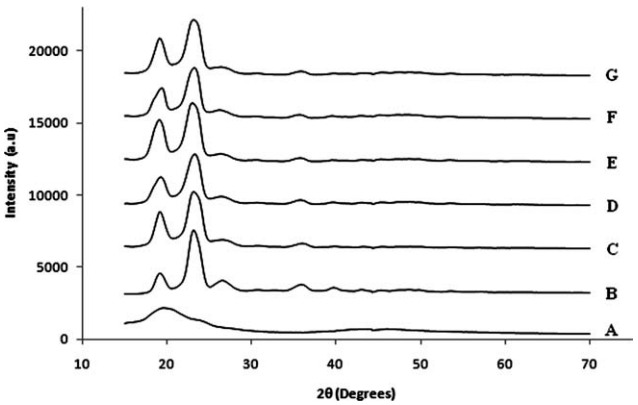

Figure 5 XRD profile of the bulk samples and developed nanofiber samples for (A) Bulk BEH-PPV, (B) Bulk PEO, (C) 0.5% BEH-PPV, (D) 1% BEH-PPV, (E) 2.5% BEH-PPV, (F) 5% BEH-PPV, and (G) 10% BEH-PPV.

CONCLUSIONS

The fabrication of hybrid BEH-PPV/PEO nanofibers using the Forcespinning™ method is reported. The resulting fibers were produced rapidly and at high yields (about 1 g min^{-1}). The relationship between spinning rpm and the fiber yield and size were established, showing a trend of decreasing fiber size with increasing rpm and a range of optimal rpm for high yields. At optimum settings, fibers with average sizes of 570 nm were obtained with 5%BEH-PPV concentration. The size of the fibers seem to be strongly dependent on the solvent used; as previously reported, pure PEO fibers showed an average diameter of 300 nm when water was used as the solvent though while using chloroform the diameter increase to 650 nm on average. This suggests that selection of a different less volatile solvent which can dissolve both PEO and BEH-PPV may produce smaller fiber diameters. BEH-PPV causes melting point depression and acts as a nucleating agent at low concentrations (0.5% to 2.5%) of BEH-PPV. The addition of BEH-PPV did not cause alteration of the crystal lattice of PEO but resulted in a slight increase in the signal intensity at ca. 20°. The fabricated fibers using conjugated polymer materials are of interest in the field of opto-electronics and can be used in the medical field, such as diagnosis and wound care, where the properties of conjugated polymers can play an important role.

The authors acknowledge Sara Farhangi and the Howard Hughes Medical Institute (HHMI) for SEM analysis at the University of Texas Pan American.

TABLE V
DSC Results

Sample	Solvent	Melt onset temp. (°C)	Melt peak temp. (°C)	Crystallization onset temp. (°C)	Crystallization peak temp. (°C)	ΔH_f (J g^{-1})
Bulk PEO	$CHCl_3$	60.5	67.4	42.5	40	251.3
0.5% BEH-PPV in PEO	$CHCl_3$	58.8	65.9	44.3	42.6	207.7
1% BEH-PPV in PEO	$CHCl_3$	58.5	65.7	44.3	41.6	210.1
2.5% BEH-PPV in PEO	$CHCl_3$	57.5	65	44.2	41.1	200.8
5% BEH-PPV in PEO	$CHCl_3$	58.9	66.8	43.1	40	189.6
10% BEH-PPV in PEO	$CHCl_3$	58.8	65.8	40	37.8	205.6

References

1. Lui, C.; Holman, Z.; Kortshagen, U. Nano Lett 2009, 9, 449.
2. Serap Gunes, H. N.; Sariciftci, N. S. Chem Rev 2007, 107, 1324.
3. Burroughes, J. H.; Bradley, D. D. C.; Brown, A. R.; Marks, R. N.; Mackay, K.; Friend, R. H.; Burns, P. L.; Holmes, A. B. Nature 1990, 347, 539.
4. Mitschke, U.; Bäuerle, P. J Mater Chem 2000, 10, 1471.
5. Sirringhaus, H.; Tessler, N.; Friend, R. H. Science 1998, 280, 1741.
6. Sirringhaus, H. Adv Mater 2005, 17, 2411.
7. Lange, U.; Roznyatovskaya, N.; Mirsky, V. Anal Chim Acta 2008, 614, 1.
8. Malhotra, B.; Chaubey, A.; Singh, S. Anal Chim Acta 2006, 578, 59.
9. Ates, M.; Sarac, A. Prog Org Coat 2009, 66, 337.
10. Wu, C.; Bull, B.; Szymanski, C.; Christensen, K.; McNeill, J. ACS Nano 2008, 2, 2415.
11. Garnier, F. Encyclopedia of Materials: Science and Technology; 2008, pp 1150–1158.
12. Guimard, N. K.; Gomez, N.; Schmidt, C. Prog Polym Sci 2007, 32, 876.
13. Gizdavic-Nikolaidis, M.; Travas-Sejdic, J.; Bowmaker, G. A.; Cooney, R. P.; Thompson, C.; Kilmartin, P. A. Curr Appl Phys 2004, 4, 347.
14. Smela, E. Adv Mater 2003, 15, 481.
15. Choi, M. C.; Kim, Y.; Ha, C. S. Prog Polym Sci 2008, 33, 581.
16. Riechel, C.; Kallinger, C.; Lemmer, U.; Feldmann, J.; Gombert, A.; Wittwer, V.; Scherf, U. Appl Phys Lett 2000, 77, 2310.
17. Vasdekis, A. Microresonators for organic semiconductor and fluidic lasers, Ph. D., University of St Andrews, UK, 2007.
18. Cortés, M.; Moreno, J. e-Polymers 2003, 041, 1.
19. Mazzoldi, A.; De Rossi, D. Proc SPIE 2000, 3987, 273.
20. Shoa, T.; Madden, J. D.; Fekri, N.; Munce, N. R.; Yang, V. X. Conf Proc IEEE Eng Med Biol Soc 2008, 2008, 2063.
21. Pettersson, P. F.; Jager, E. W. H.; Inganas, O. Presented at 1st Annual International IEEE-EMBS Special Topic Conference on Microtechnologies in Medicine & Biology, Lyon, France, Oct 12–14, 2000.
22. Jager, E.; Smela, E.; Inganas, O. Science 2000, 290, 1540.
23. Hoofman, R. J. O. M.; de Haas, M. P.; Siebbeles, L. D. A.; Warman, J. M. Nature 1998, 392, 54.
24. Babel, A.; Li, D.; Xia, Y. N.; Jenekhe, S. A. Macromolecules 2005, 38, 4705.
25. Liu, H.; Reccius, C. H.; Craighead, H. G. Appl Phys Lett 2005, 87, 253106.
26. Zhu, Z.; Zhang, L.; Smith, S.; Fong, H.; Sun, Y.; Gosztola, D. Synth Met 2009, 159, 1454.
27. Zhao, Q.; Xin, Y.; Huang, Z.; Liu, S.; Yang, C.; Li, Y. Polymer 2007, 48, 4311.
28. Li, D.; Babel, A.; Jenekhe, S.; Xia, Y. Adv Mater 2004, 16, 2062.
29. Yang. P. P.; Chen, J. F.; Huang, Z. H.; Zhan, S. M.; Jiang, Z. J.; Qiu, Y. Q.; Shao, C. Mater Lett 2009, 63, 1978.
30. Sarkar, K.; Gomez, C.; Zambrano, S.; Ramirez, M.; de Hoyos, E.; Vasquez, H.; Lozano, K. Mater Today 2010, 13, 12.
31. Osswald, T.; Hernandez-Ortiz, J. P. Polymer Processing-Modeling and Simulation; Hanser Publishers, Munich, 2006.
32. Boubnov, B. M.; Golitsyn, G. S. Convection in Rotating Fluids; Dordrecht, Boston, Kluwer Academic, 1995.
33. Neef, C. J.; Ferraris, J. P. Macromolecules 2000, 33, 2311.
34. Zepeda, D.; Guiterrez; J. J.; Ferraris, J. P. PMSE Prepr 2007, 97, 748.
35. Zepeda, D.; Gutierrez, J. J.; Ferraris, J. P. Polym Prepr 2007, 48, 45.
36. Wen, Z.; Zonghao, H.; Eryun, Y.; Cheng, W.; Yi, X.; Qiang, Z.; Yanbin, T. Mater Sci Eng 2007, 443, 292.